Emergence of Quantum Chaos in Quantum Computer Core and How to Manage It

B. Georgeot and D. L. Shepelyansky(*)
Laboratoire de Physique Quantique, UMR 5626 du CNRS, Université Paul Sabatier, F-31062 Toulouse Cedex 4, France
(May 2, 2000)

We study the standard generic quantum computer model, which describes a realistic isolated quantum computer with fluctuations in individual qubit energies and residual short-range inter-qubit couplings. It is shown that in the limit where the fluctuations and couplings are small compared to one-qubit energy spacing the spectrum has a band structure and a renormalized Hamiltonian is obtained which describes the eigenstate properties inside one band. The studies are concentrated on the central band of the computer ("core") with the highest density of states. We show that above a critical inter-qubit coupling strength, quantum chaos sets in, leading to quantum ergodicity of the computer eigenstates. In this regime the ideal qubit structure disappears, the eigenstates become complex and the operability of the computer is quickly destroyed. We confirm that the quantum chaos border decreases only linearly with the number of qubits n, although the spacing between multi-qubit states drops exponentially with n. The investigation of time-evolution in the quantum computer shows that in the quantum chaos regime, an ideal (noninteracting) state quickly disappears and exponentially many states become mixed after a short chaotic time scale for which the dependence on system parameters is determined. Below the quantum chaos border an ideal state can survive for long times and be used for computation. The results show that a broad parameter region does exist where the efficient operation of a quantum computer is possible.

PACS numbers: 03.67.Lx, 05.45.Mt, 24.10.Cn

I. INTRODUCTION

During the last decade, a remarkable progress has been achieved in the fundamental understanding of the main elements necessary for the creation of a quantum computer. Indeed, as stressed by Feynman [1], classical computers have tremendous problems to simulate very common quantum systems, since the computation time grows exponentially with the number of quantum particles. Therefore for such problems it is natural to envision a computer composed from quantum elements (qubits) which operate according to the laws of quantum mechanics. In any case, such devices will be in a sense unavoidable since the technological progress leads to chips of smaller and smaller size which will eventually reach the quantum scale. At present a quantum computer is viewed as a system of n qubits (two-level quantum systems), with the possibility of switching on and off a coupling between them (see the detailed reviews in [2–4]). The operation of such computers is based on reversible unitary transformations in the Hilbert space whose dimension $N_H = 2^n$ is exponentially large in n. It has been shown that all unitary operations can be realized with two-qubit transformations [5,6]. This makes necessary the existence of a coupling between qubits. Any quantum algorithm will be a sequence of such fundamental transformations, which form the basis of a new quantum logic.

An important next step was the discovery of quantum algorithms which can make certain computations much faster than on a classical computer. The most impressive is the problem of factorization of large numbers in prime factors, for which Shor constructed [7] a quantum algorithm which is exponentially faster than the classical ones. It was also shown by Grover [8] that the searching of an item in a long list is parametrically much faster on a quantum computer. The recent development of error-correcting codes [9,10] showed that a certain amount of noise due to external coupling could be tolerable in the operation of a quantum computer.

All these exciting developments motivated a great body of experimental proposals to effectively realize such a quantum computer. They include ion traps [11], nuclear magnetic resonance systems [12], nuclear spins with interaction controlled electronically [13,14] or by laser pulses [15], quantum dots [16], Cooper pair boxes [17], optical lattices [18] and electrons floating on liquid helium [19]. As a result, a two-qubit gate has been experimentally realized with cold ions [20], and the Grover algorithm has been performed for three qubits made from nuclear spins in a molecule [21]. However, to have a quantum computer competitive with a classical one will require a much larger number of qubits. For example, the minimal number of qubits for which Shor's algorithm will become useful is of the order of $n = 1000$ [4]. As a result, a great experimental effort is still needed on the way to quantum computer realization.

A serious obstacle to the physical realization of such computers is the quantum decoherence due to the couplings with the external world which gives a finite lifetime to the excited state of a given qubit. This question has been discussed by several groups for different experimental qubit realizations [4,6,22,23]. The effects of decoherence and laser pulse shape broadening were

numerically simulated in the context of Shor's algorithm [24,25], and shown to be quite important for the operability of the computer. However, in a number of physical proposals, for example nuclear spins in two-dimensional semiconductor structures, the relaxation time due to this decoherence process can be many orders of magnitude larger than the time required for the gates operation [2,13,14,23], so that there are hopes to manage this obstacle.

Here we will focus on a different obstacle to the physical realization of quantum computers that was not stressed up to now. This problem arises even if the decoherence time is infinite and the system is isolated/decoupled from the external world. Indeed, even in the absence of decoherence there are always imperfections in physical systems. Due to that the spacing between the two states of each qubit will fluctuate in some finite detuning interval δ. Also, some residual static interaction J between qubits will be unavoidably present (we remind that an inter-qubit coupling is required to operate the gates). Extensive studies of many-body interacting systems such as nuclei, complex atoms, quantum dots and quantum spin glasses [26–35] have shown that generically in such systems the interaction leads to quantum chaos characterized by ergodicity of the eigenstates and level spacing statistics as in Random Matrix Theory (RMT) [36,37]. In a sense the interaction leads to dynamical thermalization without coupling to an external thermal bath. If the quantum computer were in such a regime, its operability would be effectively destroyed since the noninteracting multi-qubit states representing the quantum register states will be eliminated by quantum ergodicity.

In this respect, it is important to stress that unavoidably the residual interaction J will be much larger than the energy spacing Δ_n between adjacent eigenstates of the quantum computer. Indeed the residual interaction J is relatively small so that all N_H computer eigenenergies are distributed in an energy band of size $\Delta E \sim n\Delta_0$, where Δ_0 is the average energy distance between the two levels of one qubit and n is the total number of qubits in the computer. As a consequence, the spacing between multi-qubit states is $\Delta_n \approx \Delta E/N_H \sim n\Delta_0 2^{-n} \ll \Delta_0$. Let us consider a realistic estimate for Δ_n and J for the case with $n = 1000$ as required for Shor's algorithm to be useful. For $\Delta_0 \sim 1$ K, which corresponds to the typical one-qubit spacing in the experimental proposals [13,14], the multi-qubit spacing becomes $\Delta_n \sim 10^3 \times 2^{-10^3}\Delta_0 \sim 10^{-298}$ K. This value will definitely be much smaller than any physical residual interaction. In the case of the proposal [14], for example, with a distance between donors of $r = 200$ Å and an effective Bohr radius of $a_B = 30$ Å (Eq.(2) of [14]), the coupling between qubits (spin-spin interaction) is $J \sim \Delta_0 \sim 1$ K. By changing the electrostatic gate potential, the effective electron mass can be modified up to a factor of two. Since $J \propto (r/a_B)^{5/2}\exp(-2r/a_B)/a_B$, and a_B is inversely proportional to the effective mass, this gives a minimal residual spin-spin interaction of $J \sim 10^{-5}$ K $\gg \Delta_n$. In this situation, one would naturally/naively expect that level mixing, quantum ergodicity of eigenstates and chaos are unavoidable since the interaction is much bigger than the energy spacing between adjacent levels ($J \gg \Delta_n$).

In spite of this natural expectation, it was shown recently in [38] that in the quantum computer the quantum chaos sets in only for couplings J exponentially stronger than Δ_n. In fact, it was shown that the critical coupling J_c for the transition to quantum chaos decreases only linearly with the number of qubits n (for short-range inter-qubit coupling): $J_c \sim \Delta_0/n$. This result opens a broad parameter region where a quantum computer can be operated below the quantum chaos border, when noninteracting multi-qubit states are very close to the exact quantum computer eigenstates. For example, at $n = 1000$ and $\Delta_0 \sim 1$ K, the critical residual interaction is $J_c \sim 1$ mK, compatible with the proposal discussed above [14].

In the present paper, we study in more details the transition to chaos and how it affects the time evolution of the system. The effects of residual interaction in the presence or absence of fine fluctuations of individual qubit energy spacing are analyzed in great detail. The paper is composed as follows. In the next section we describe the standard generic quantum computer (SGQC) model, introduced in [38]. In section III, we present the result of numerical and analytical studies of eigenenergies and eigenstate properties of this model. Section IV is devoted to the analysis of the time evolution of this system, and the typical time scales for the development of quantum chaos are presented as a function of the system parameters. We end by some concluding remarks in the last section.

II. STANDARD GENERIC QUANTUM COMPUTER MODEL

In [38] the standard generic quantum computer (SGQC) model was introduced to describe a system of n qubits containing imperfections which generate a residual inter-qubit coupling and fluctuations in the energy spacings between the two states of one qubit. The Hamiltonian of this model reads:

$$H = \sum_i \Gamma_i \sigma_i^z + \sum_{i<j} J_{ij}\sigma_i^x\sigma_j^x, \qquad (1)$$

where the σ_i are the Pauli matrices for the qubit i and the second sum runs over nearest-neighbor qubit pairs on a two-dimensional lattice with periodic boundary conditions applied. The energy spacing between the two states of a qubit is represented by Γ_i randomly and uniformly

distributed in the interval $[\Delta_0 - \delta/2, \Delta_0 + \delta/2]$. The detuning parameter δ gives the width of the distribution near the average value Δ_0 and may vary from 0 to Δ_0. Fluctuations in the values of Γ_i appear generally as a result of imperfections. For example, in the frame of the experimental proposals [13,14], the detuning δ will appear for nuclear spin levels as a result of local magnetic fields and density fluctuations. For electrons floating on liquid helium [19], it will appear due to fluctuations of the electric field near the surface. The couplings J_{ij} represent the residual static interaction between qubits which is always present for reasons explained in the introduction. They can originate from spin-exciton exchange [13,14], Coulomb interaction [11], dipole-dipole interaction [19], etc... To catch the general features of the different proposals, we chose J_{ij} randomly and uniformly distributed in the interval $[-J, J]$. We note that a similar Hamiltonian, but without coupling/detuning fluctuations, was discussed for a quantum computer based on optical lattices [18,39]. This SGQC model describes the quantum computer hardware, while the gate operation in time should include additional time-dependent terms in the Hamiltonian (1) and will be studied separately. At $J = 0$ the noninteracting eigenstates of the SGQC model can be presented as $|\psi_i >= |\alpha_1, ..., \alpha_n >$ where $\alpha_k = 0, 1$ marks the polarization of each individual qubit. These are the ideal eigenstates of a quantum computer, and we will call them quantum register states. For $J \neq 0$, these states are no longer eigenstates of the Hamiltonian, and the new eigenstates are now linear combinations of different quantum register states. We will use the term multi-qubit states to denote the eigenstates of the SGQC model with interaction but also for the case $J = 0$.

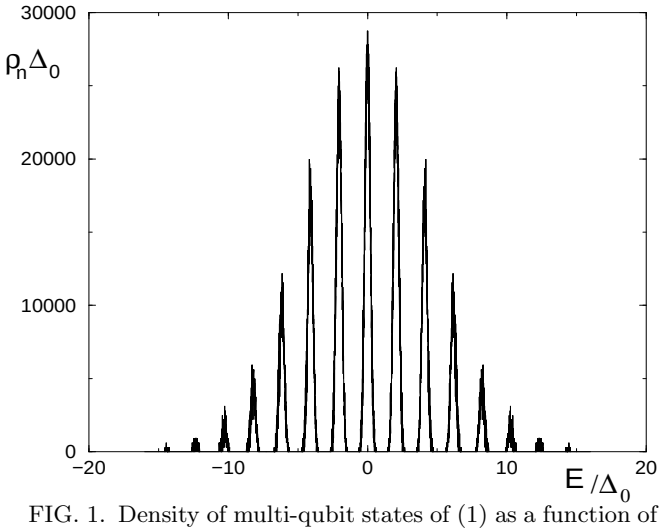

FIG. 1. Density of multi-qubit states of (1) as a function of total system energy E for $J = 0$. Here $n = 16$ and $\delta/\Delta_0 = 0.2$. The two extreme bands at $E/\Delta_0 \approx \pm 16$ contain only one state and are not seen at this scale.

While in [38] the main studies were concentrated on the case where δ is relatively large and comparable to Δ_0, here we will focus on the case $\delta \ll \Delta_0$, which corresponds to the situation where fluctuations induced by imperfections are relatively weak. In this case, the unperturbed energy spectrum of (1) (corresponding to $J = 0$) is composed of $n + 1$ well separated bands, with interband spacing $2\Delta_0$. An example of the density of multi-qubit states $\rho_n = 1/\Delta_n$ in this situation is presented in Fig.1. Since the Γ_i randomly fluctuate in an interval of size δ, each band at $J = 0$, except the extreme ones, have a Gaussian shape with width $\approx \sqrt{n}\delta$. The number of states inside a band is approximately N_H/n, so that the energy spacing between adjacent multi-qubit states inside one band is exponentially small ($\delta_n \sim n^{3/2}2^{-n}\delta$), in line with the general estimate in Section I.

In the presence of a residual interaction $J \sim \delta$, the spectrum will still have the above band structure with exponentially large density of states. For $J \sim \delta \ll \Delta_0$, the interband coupling is very weak and can be neglected. In this situation, the SGQC Hamiltonian (1) is to a good approximation described by the renormalized Hamiltonian $H_P = \Sigma_{k=1}^{n+1} \hat{P}_k H \hat{P}_k$ where $\hat{P}_k$ is the projector on the k^{th} band, so that qubits are coupled only inside one band. We will thereafter concentrate our studies on the band nearest to $E = 0$. For an even n this band is centered exactly at $E = 0$, while for odd n there are two bands centered at $E = \pm\Delta_0$, and we will use the one at $E = -\Delta_0$. Such a band corresponds to the highest density of states, and in a sense represents the quantum computer core. It is clear that quantum chaos and ergodicity will first appear in this band, which will therefore set the limit for operability of the quantum computer. Inside this band, the system is described by a renormalized Hamiltonian H_P which depends only on the number of qubits n and the dimensionless coupling J/δ.

III. QUANTUM COMPUTER EIGENENERGIES AND EIGENSTATES

The first investigations in [38] showed that the quantum chaos border in the SGQC model (1) corresponds to a critical interaction J_c given by:

$$J_c \approx \frac{C\delta}{n}, \tag{2}$$

where C is a numerical constant. This border is exponentially larger than the energy spacing between adjacent multi-qubit states Δ_n. The physical origin of this difference is due to the fact that the interaction is of a two-body nature. As a result, one noninteracting multi-qubit state $|\psi_i >$ has nonzero coupling matrix elements only with $2n$ other multi-qubit states. In the basis of quantum register states $|\psi_i >$, the Hamiltonian is represented by a very sparse nondiagonal matrix with only $2n+1$ nonzero matrix elements by line of length $N_H = 2^n$. For $\delta \approx \Delta_0$

all these transitions take place in an energy interval B of width of order $6\Delta_0$. Therefore the energy spacing between directly coupled states is $\Delta_c \approx B/2n \approx 3\Delta_0/n$. According to the studies of quantum chaos in many-body systems [27,30–35,38], the transition to chaos takes place when the matrix elements become larger than the energy spacing between directly coupled states. This gives $J > \Delta_c$ which leads to the relation (2). For the case $\delta \ll \Delta_0$ on which we focus here, still in the renormalized Hamiltonian H_P the number of nonzero matrix elements in one line is of the order of n, and $B \sim \delta$, so that $\Delta_c \sim \delta/n$, that leads to the result (2) [40].

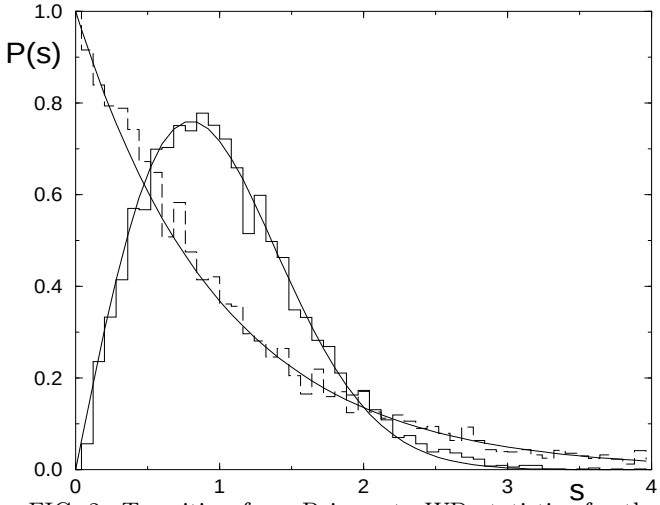

FIG. 2. Transition from Poisson to WD statistics for the renormalized Hamiltonian of SGQC model in the central band. The statistics is obtained for the states in the middle of the energy band (±6.25% around the center) for n=16 : $J/\delta = 0.05, \eta = 0.99$ (dashed line histogram); $J/\delta = 0.32, \eta = 0.047$ (full line histogram). Full curves show the Poisson distribution $P_P(s)$ and the Wigner-Dyson distribution $P_W(s)$; $N_D = 8$, $N_S > 1.2 \times 10^4$.

The transition to quantum chaos and ergodicity can be clearly seen in the change of the spectral statistics of the system. One of the most convenient is the level spacing statistics $P(s)$, which gives the probability to find two adjacent levels whose spacing is in $[s, s + ds]$. Here s is the energy spacing measured in units of average level spacing. It is well known that while the average density of states is not sensitive to the presence or absence of chaos, the fluctuations of the energy spacings between adjacent levels around the mean value, determined by $P(s)$, are sensitive to it. In the presence of chaos, eigenstates are ergodic, overlap of wavefunctions gives a finite coupling matrix element between nearby states and the spectral statistics $P(s)$ follows the Wigner-Dyson (WD) distribution $P_W(s) = (\pi s/2)\exp(-\pi s^2/4)$ typical for random matrices. This distribution $P_W(s)$ shows level repulsion at small s, due to the fact that overlap matrix elements between adjacent levels tend to move them away from each other. On the contrary, in the integrable case at $J \ll J_c$, the overlap coupling matrix element between nonergodic states is very small. As a result, energy levels are uncorrelated and $P(s)$ follows the Poisson distribution $P_P(s) = \exp(-s)$ known to be valid for integrable one-particle systems [36].

In the SGQC model, we expect a transition from $P_P(s)$ at small J to $P_W(s)$ above the quantum chaos border (2). An example of such a transition is shown in Fig.2. To decrease the statistical fluctuations we averaged over several independent realizations of the Γ_i and J_{ij} in (1), which is the standard procedure used in Random Matrix Theory [36,37]. We used up to $N_D = 5 \times 10^4$ realizations so that the total statistics $1.5 \times 10^5 \geq N_S > 1.2 \times 10^4$. It is interesting to note that in the limit $J/\delta \to \infty$ ($\delta \ll J \ll \Delta_0$) the system remains in the regime of quantum chaos with WD statistics [41], as is illustrated in Fig.3. This means that in the absence of individual qubit energy fluctuations, the residual coupling alone leads to chaotic eigenstates.

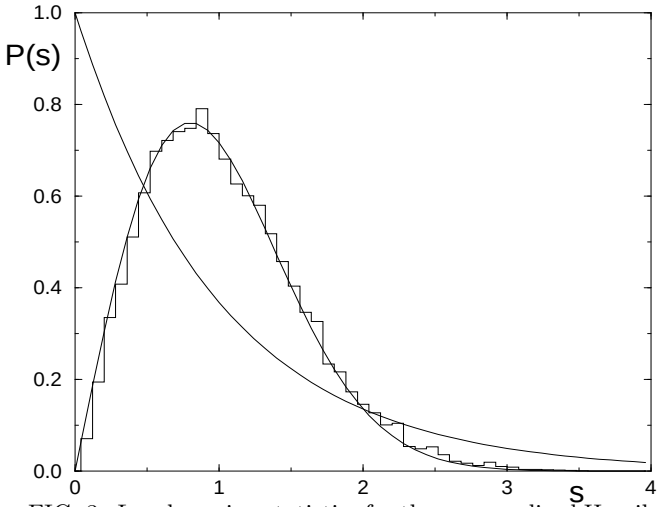

FIG. 3. Level spacing statistics for the renormalized Hamiltonian of SGQC model in the central band for $\delta = 0$. The statistics is obtained for the states in the middle of the energy band (±6.25% around the center) for n=15 : $\eta = 0.023$ (histogram). Full curves show $P_P(s)$ and $P_W(s)$; $N_D = 20$, $N_S > 1.6 \times 10^4$.

To characterize the variation of $P(s)$ from one limiting distribution to another it is convenient to use the parameter $\eta = \int_0^{s_0}(P(s) - P_W(s))ds / \int_0^{s_0}(P_P(s) - P_W(s))ds$ [31], where $s_0 = 0.4729...$ is the intersection point of $P_P(s)$ and $P_W(s)$. In this way $P_P(s)$ corresponds to $\eta = 1$, and $P_W(s)$ to $\eta = 0$. The studies of different systems has already shown that this parameter characterizes well the transition from one statistics to the other [31,33,35,38]. Indeed, according to the data of Fig.4, η changes from 1 at small J to $\eta \approx 0$ at large J. To characterize this transition, we chose the critical value J_c by the condition $\eta(J_c) = 0.3$. The dependence of η on the rescaled coupling strength J/J_c shows that the transition becomes

sharper and sharper when n increases (Fig.4).

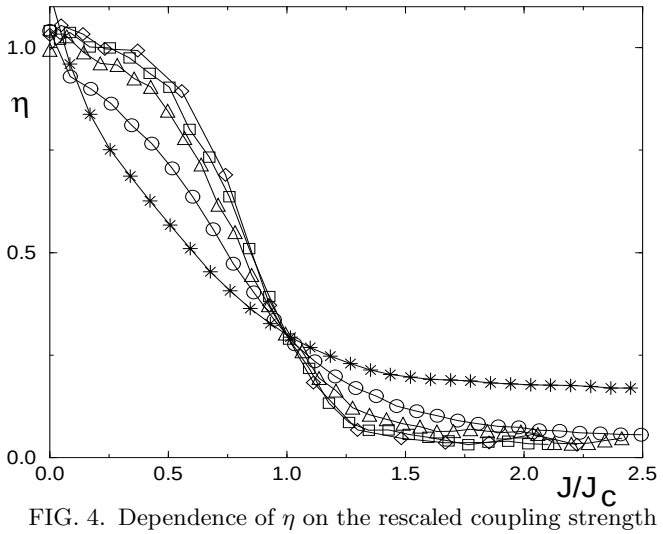

FIG. 4. Dependence of η on the rescaled coupling strength J/J_c for the states in the middle of the energy band for $n = 6(*), 9(\mathrm{o}), 12(\mathrm{triangles}), 15(\mathrm{squares}), 16(\mathrm{diamonds})$.

The dependence of the critical coupling strength J_c on the number of qubits n is shown on Fig.5. It clearly shows that this critical strength decreases linearly with n and follows the theoretical border (2) with $C \approx 3$. For comparison on the same figure we also show the dependence of the multi-qubit spacing Δ_n (computed numerically) on n. It definitely demonstrates that $J_c \gg \Delta_n$.

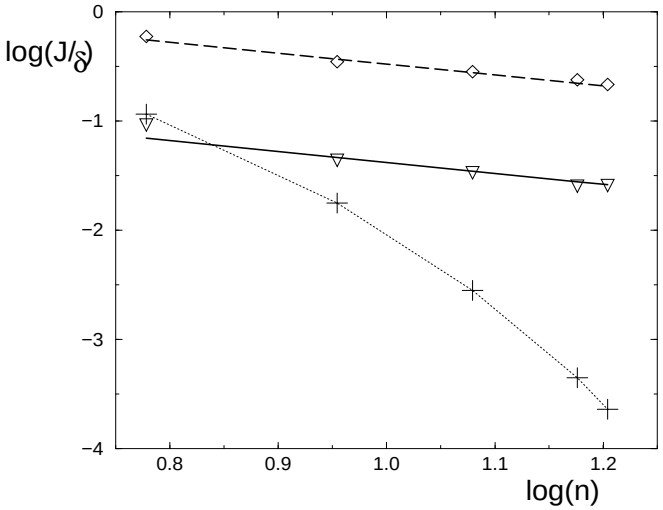

FIG. 5. Dependence of $\log(J_c/\delta)$ (diamonds) and $\log(J_{cs}/\delta)$ (triangles) versus $\log(n)$; the variation of the scaled multi-qubit spacing ($\log(\Delta_n/\delta)$) with $\log(n)$ is shown for comparison (+). Dashed line gives the theoretical formula $J_c = C\delta/n$ with $C = 3.3$; the solid line is $J_{cs} = 0.41\delta/n$; the dotted curve is drawn to guide the eye for (+).

The transition in the level spacing statistics reflects a qualitative change in the structure of the eigenstates. While for $J \ll J_c$ the eigenstates are expected to be very close to the quantum register states $|\psi_i>$, for $J > J_c$ each eigenstate $|\phi_m>$ becomes a superposition of an exponential number of states $|\psi_i>$. It is convenient to characterize the complexity of an eigenstate $|\phi_m>$ by the quantum eigenstate entropy $S_q = -\sum_i W_{im} \log_2 W_{im}$, where W_{im} is the quantum probability to find the quantum register state $|\psi_i>$ in the eigenstate $|\phi_m>$ of the Hamiltonian ($W_{im} = |<\psi_i|\phi_m>|^2$). In this way $S_q = 0$ if $|\phi_m>$ is one quantum register state ($J = 0$), $S_q = 1$ if $|\phi_m>$ is equally composed of two $|\psi_i>$, and the maximal value is $S_q = n$ if all 2^n states contribute equally to $|\phi_m>$. We average S_q over the states in the center of the energy band and N_D realizations of Γ_i and J_{ij}.

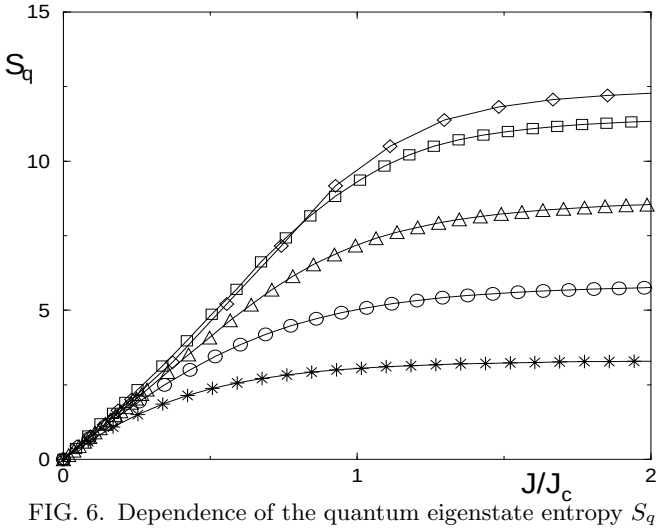

FIG. 6. Dependence of the quantum eigenstate entropy S_q on J/J_c for $n = 6(*)$, 9 (o), 12 (triangles), 15 (squares), 16 (diamonds); $1.5 \times 10^5 \geq N_S > 1.2 \times 10^4$.

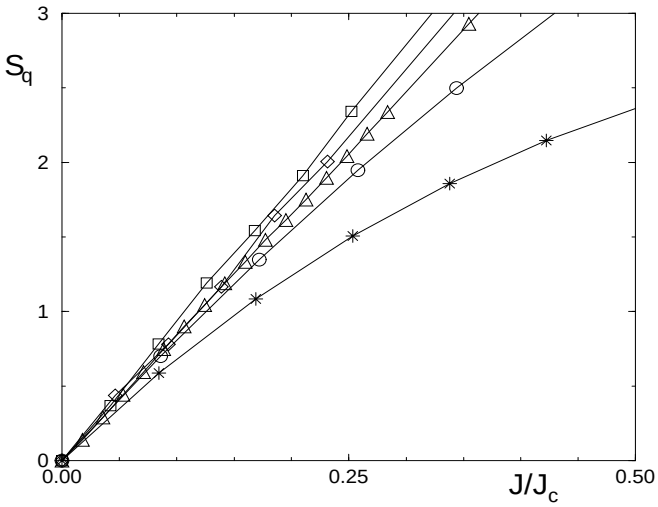

FIG. 7. Same as Fig.6 but on a larger scale.

The variation of this average S_q as a function of J for different values of n is shown on Figs.6,7. It shows that indeed the entropy S_q grows with J until it saturates to a large value corresponding to an exponential number of

mixed states. These data show that the critical coupling J_{cs} at which $S_q = 1$ (two states mixed) is proportional to J_c. Indeed, Fig.7 shows a small dispersion near $S_q = 1$ when n changes from 6 to 16, while Δ_n varies by three orders of magnitude. This is confirmed by the data on Fig.5, which give $J_{cs} \approx 0.13 J_c \approx 0.4\delta/n$. This result is in agreement with the results [38] obtained by direct diagonalization of the SGQC model (1) at $\delta \ll \Delta_0$ (lower insert in Fig.2 of [38]).

The quantum eigenstate entropy S_q characterizes the global properties of the eigenstates, while a more detailed information about them can be obtained from the local density of states ρ_W introduced by Wigner [42]:

$$\rho_W(E - E_i) = \sum_m W_{im} \delta(E - E_m) \qquad (3)$$

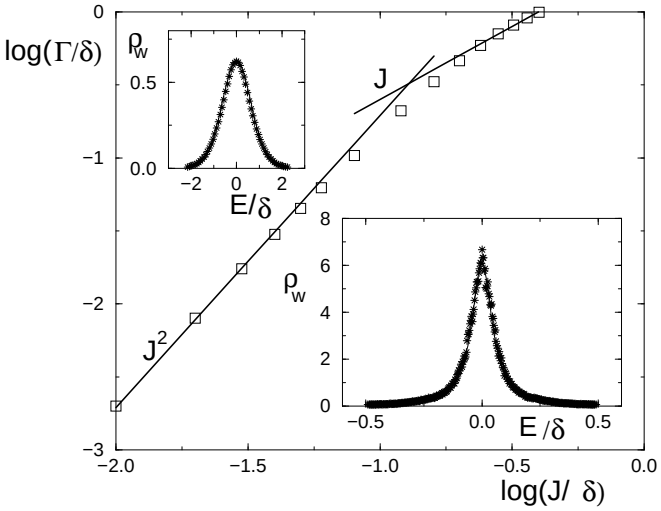

FIG. 8. Dependence of the Breit-Wigner width Γ on the coupling strength J for $n = 15$ for the states in the middle of the energy band. The straight lines show the theoretical dependence (5) with $\Gamma = 1.3 J^2 n/\delta$ and the strong coupling regime with $\Gamma \sim J$; $N_D = 20$. Lower insert: example of the local density of states ρ_W (3) for $J/\delta = 0.08$; the full line shows the best fit of the Breit-Wigner form (4) with $\Gamma = 0.10\delta$. Upper insert: example of the local density of states ρ_W (3) for $J/\delta = 0.4$; the full line shows the best Gaussian fit of width $\Gamma = 0.64\delta$.

The function ρ_W characterizes the average probability distribution of W_{im} (see a numerical example in Fig.3 of [38]). For moderate coupling strength, ρ_W is well described by the well-known Breit-Wigner distribution $\rho_W = \rho_{BW}$:

$$\rho_{BW}(E - E_i) = \frac{\Gamma}{2\pi((E - E_i)^2 + \Gamma^2/4)} \qquad (4)$$

where Γ is the width of the distribution. This expression is valid when Γ is smaller than the bandwidth ($\Gamma < \sqrt{n}\delta$) and many levels are contained inside this width. In this regime, the Breit-Wigner width Γ is given by the Fermi golden rule: $\Gamma = 2\pi U_s^2 \rho_c$, where U_s is the root mean square of the transition matrix element and ρ_c is the density of directly coupled states. The validity of this formula was well checked in many-body systems with quantum chaos [28,33,34,37]. In our case $U_s \sim J$ and $\rho_c \sim n/\delta$, so that:

$$\Gamma \sim \frac{J^2 n}{\delta}. \qquad (5)$$

This dependence is confirmed by the data on Fig.8. However, for large J, when $\Gamma > \sqrt{n}\delta$, the shape of ρ_W becomes non-Lorentzian and is well fitted by a Gaussian distribution. The width of this modified distribution grows like $\Gamma \sim J$. This scaling naturally appears in the limit $\delta = 0$, $J \ll \Delta_0$, since the noninteracting part of the Hamiltonian is simply a constant commuting with the perturbation. The change from one dependence to the other takes place for $J > \delta/n^{1/4}$. Above this limit Γ is still weakly dependent on the number of qubits n. We expect that for $J \gg \delta$ the energy width of one band is $\Gamma \sim J\sqrt{n}$ (effective frequency of n Rabi frequencies with random signs), and have checked numerically this law for $\delta = 0$ (data not shown).

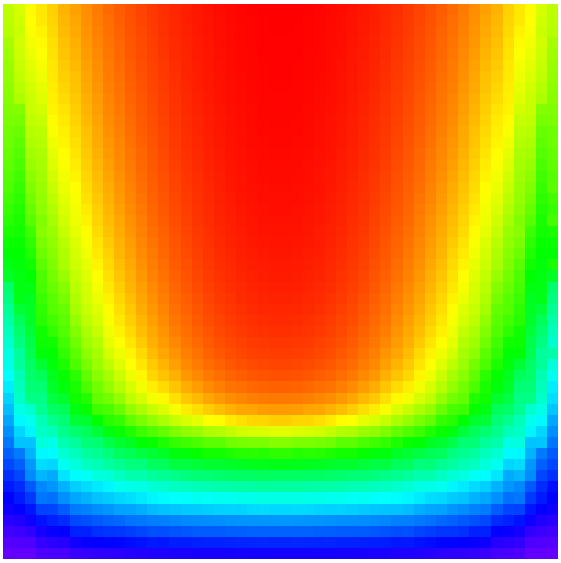

FIG. 9. Melting of the quantum computer core generated by the inter-qubit coupling. Color represents the level of quantum eigenstate entropy S_q, from bright red ($S_q \approx 12$) to blue ($S_q = 0$). Horizontal axis is the scaled energy E/δ of the computer eigenstates in the central band counted from the band bottom to the top ($E/\delta \approx \pm\sqrt{n}$). Vertical axis is the value of J/δ, varying from 0 to 0.5. Here $n = 16$, $J_c/\delta = 0.22$, and one random realization is chosen.

According to the results obtained from many-body systems [33], the number of quantum register states mixed inside the width Γ is of the order of $\Gamma\rho_n$, and is exponentially large. This however assumes that $J > J_c$ and the system is already in the quantum chaos regime.

In this case the quantum eigenstate entropy S_q is large ($S_q \approx \log_2(\Gamma\rho_n) \sim n$) and the operability of the computer is quickly destroyed, since many quantum register states become mixed. The pictorial view of the quantum computer melting is shown on Fig.9. This image is qualitatively similar to the one in [38] (Fig.5 there), which was obtained for the SGQC model at $\delta = \Delta_0$. In Fig.9 the melting goes in a smoother way since all the states belong to the same central band (quantum computer core).

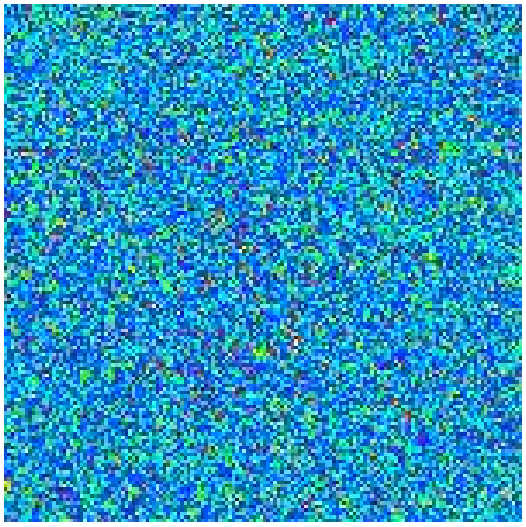

FIG. 10. Quantum chaos in the quantum register: color represents the value of the projection probability W_{im} of the quantum register states on the eigenstates of the Hamiltonian, from bright red (maximal value)to blue (minimal value). Horizontal axis corresponds to 150 quantum register states, the vertical axis represents the 150 computer eigenstates (both ordered in energy). Here $n = 16$, $J/\delta = 0.4$ ($J/\delta > J_c/\delta = 0.22$), and one random realization is chosen.

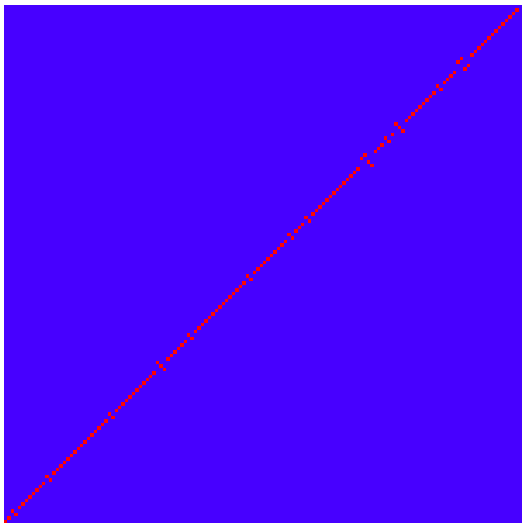

FIG. 11. Same as Fig.10 below the quantum chaos border, $J/\delta = 0.001$ ($J/\delta \ll J_{cs}/\delta = 0.026$).

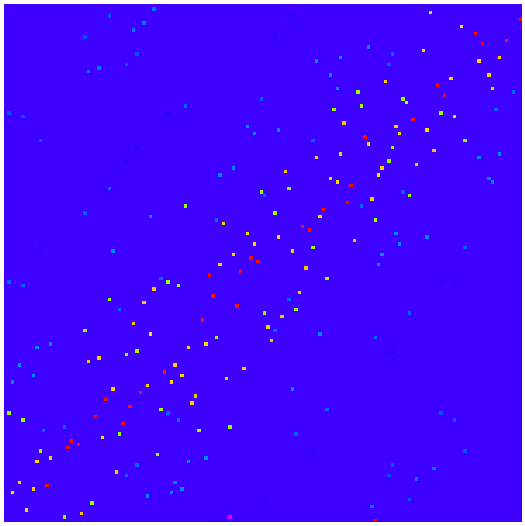

FIG. 12. Same as Fig.10 for $J/\delta = 0.01$ ($J/\delta \sim J_{cs}/\delta = 0.026$)

The effect of quantum chaos melting in the quantum register representation is shown on Fig.10 for $J > J_c$. The ideal register structure is manifestly washed out. On the contrary, below the chaos border ($J < J_c$), only few quantum register states are mixed. For comparison, Fig.11 shows the same part of the register in the regime $J \ll J_{cs}$ (no mixing of states) and Fig.12 in the regime $J \sim J_{cs}$ (few states are mixed).

IV. TIME EVOLUTION IN THE SGQC MODEL

In the previous section we determined the properties of eigenstates of the quantum computer in the presence of residual inter-qubit coupling. In the presence of this coupling the quantum register states $|\psi_i>$ are not any more stationary states, and therefore it is natural to analyze how they evolve in time. Indeed, if at time $t = 0$ an initial state is $|\chi(t=0)>=|\psi_{i_0}>$ corresponding to the quantum register state i_0, then with time the probability will spread over the register and at a time t the projection probability on the register state $|\psi_i>$ will be:

$$F_{ii_0}(t) = |<\psi_i|\chi(t)>|^2 \\ = \sum_{m,m'} A_{im} A^*_{i_0 m} A^*_{im'} A_{i_0 m'} \exp(i(E_{m'} - E_m)t), \quad (6)$$

where $A_{im} =<\psi_i|\phi_m>$ and E_m is the energy of the stationary state $|\phi_m>$ and we chose $\hbar = 1$. For $J \ll J_c$, the probability $F_{i_0 i_0}(t)$ is very close to one for all times since the states are not mixed by the interaction. This means that all quantum register states $|\psi_i>$ remain well defined, and the computer can operate properly. For $J \sim J_{cs}$, only few states $|\psi_i>$ are mixed by the interaction, and $F_{i_0 i_0}(t)$ oscillates in time regularly around an average value of order 1/2. These oscillations are similar to the Rabi oscillations between two levels with frequency $\Omega \sim J$. An example is presented in Fig.13. In this regime, we

expect that error-correcting codes [9,10] may efficiently correct the spreading over few quantum register states.

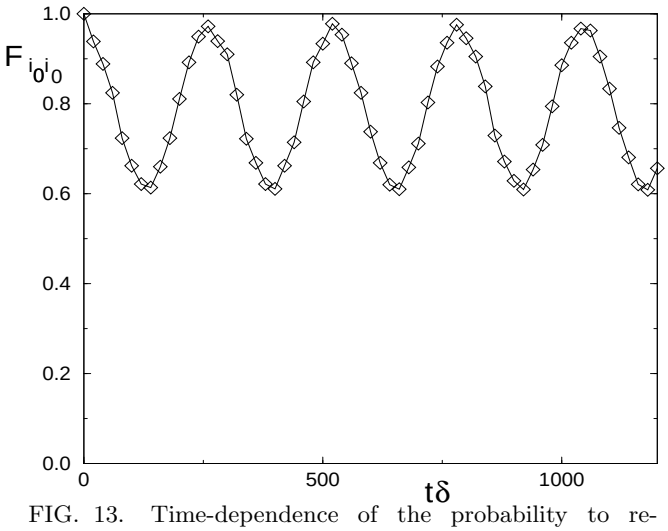

FIG. 13. Time-dependence of the probability to remain in the same quantum register state for $n = 16$, $J = 0.01 \sim J_{cs} = 0.026$ ($J_c/\delta = 0.22$) and one random realization is chosen.

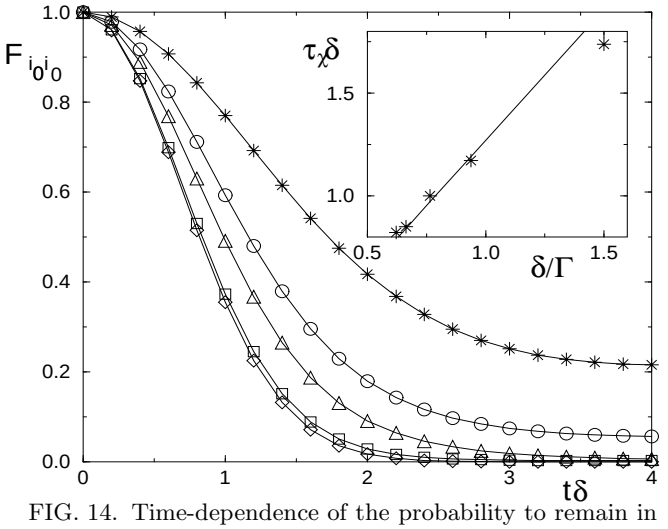

FIG. 14. Time-dependence of the probability to remain in the same quantum register state for $J/\delta = 0.4 \gg J_c/\delta$. Data are shown for $n = 16$ (diamonds, $J_c/\delta = 0.22$); $n = 15$ (squares, $J_c/\delta = 0.24$); $n = 12$ (triangles, $J_c/\delta = 0.28$); $n = 9$ (circles, $J_c/\delta = 0.35$); $n = 6$ (stars, $J_c/\delta = 0.59$). Average is made over 200 states randomly chosen in the central band. Insert shows the chaotic time scale τ_χ (defined by $F_{i_0 i_0}(\tau_\chi) = 1/2$) as a function of $1/\Gamma$; the straight line is $\tau_\chi = 1.27/\Gamma$.

For $J > J_{cs}$, quantum chaos sets in, and with time the probability spreads over more and more quantum register states until a quasi-stationary regime is reached where an exponentially large number of states are mixed. The probability $F_{i_0 i_0}(t)$ drops approximately to zero, as shown on Fig.14. The chaotic time scale for this decay τ_χ can be estimated as $\tau_\chi \sim 1/\Gamma$ where Γ is the width determined in the previous section. This estimate is very natural in the Fermi golden rule regime, with Breit-Wigner local density of states (4), since $F_{i_0 i_0}(t)$ is essentially the Fourier transform of the local density of states ρ_W, and therefore decreases as $\exp(-\Gamma t)$. We note that the decay in this regime was recently discussed in [43]. According to our data, when Γ becomes comparable to the energy bandwidth $\sqrt{n}\delta$, ρ_W is close to a Gaussian distribution of width Γ, and its Fourier transform $F_{i_0 i_0}(t)$ is also a Gaussian of width $1/\Gamma$. Therefore in both regimes we expect the time scale τ_χ for the decay of $F_{i_0 i_0}(t)$ to be $\tau_\chi \sim 1/\Gamma$. The data shown on Fig.14 correspond to the saturation regime for large values of n, and the insert shows that $\tau_\chi \sim 1/\Gamma$ is still valid. In fact the curve for $n = 16$ in Fig.14 is already close to the limiting decay curve at $\delta = 0$ (data not shown).

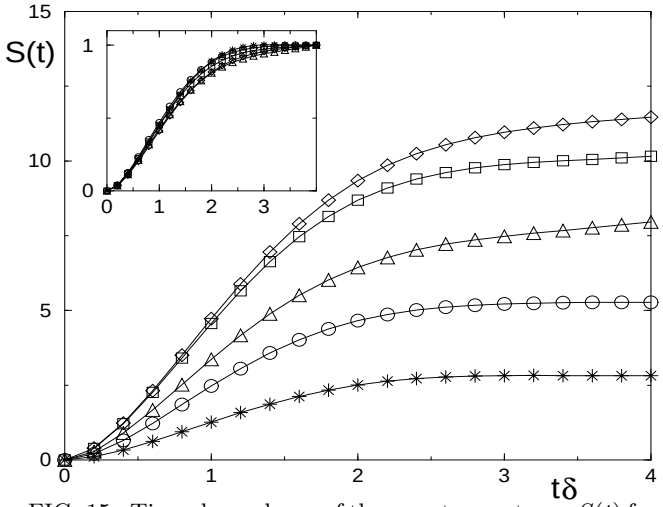

FIG. 15. Time-dependence of the quantum entropy $S(t)$ for $J/\delta = 0.4 \gg J_c/\delta$; symbols are as in Fig.14. Average is made over 200 initial states randomly chosen in the central band. Insert shows the same curves normalized to their maximal value.

At the same time scale τ_χ the quantum entropy $S(t)$ is large but is still growing. It reaches its maximal value on a larger time scale which seems independent of n. At this stage, an initial quantum register state is now spread over most of the register (Here $S(t) = -\sum_i F_{ii_0}(t) \log_2 F_{ii_0}(t)$). This process is shown on Fig.15. This maximal value of $S(t)$ is approximately given by S_q (see Fig.6) and accordingly decreases with decreasing J as is illustrated in Fig.16.

Fig.17 illustrates this mixing process in the quantum register representation, evolving in time. The quantum computer hardware becomes quickly destroyed due to the inter-qubit coupling. It is necessary to decrease the coupling strength below the quantum chaos border to get well-defined quantum register states for $t > 0$, as is illustrated in Fig.18.

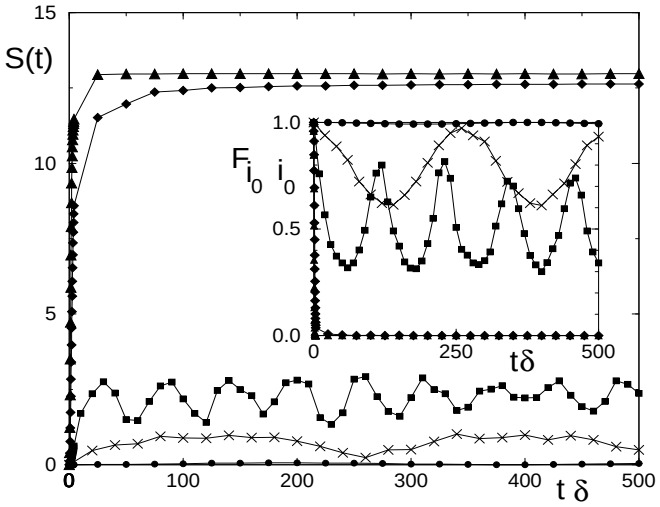

FIG. 16. Time-dependence of the quantum entropy $S(t)$ for different values of J, $n = 16$ $J_c/\delta = 0.22$, $J_{cs}/\delta = 0.026$, and one random realization is chosen: $J/\delta = 0.001 \ll J_{cs}/\delta$ (disks); $J/\delta = 0.01 < J_{cs}/\delta$ (crosses); $J/\delta = 0.03 \approx J_{cs}/\delta$ (squares); $J/\delta = 0.2 \approx J_c/\delta$ (diamonds); $J/\delta = 0.4 > J_c/\delta$ (triangles). Insert gives the probability to remain in the same quantum register state for the same values of J/δ. Averages are made over 200 states randomly chosen in the central band.

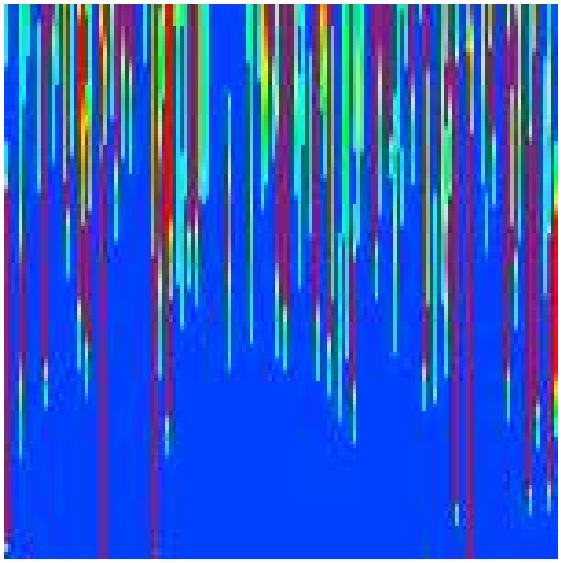

FIG. 17. Time explosion of quantum chaos in the quantum register: color represents the value of the projection probability $| < \psi_i|\chi(t) > |^2$ of an initial state on the quantum register states ordered in energy, from bright red (maximal value)to blue (minimal value). Horizontal axis corresponds to 150 states, the vertical axis to 150 time steps, from $t\delta = 0$ to $t\delta = 2$. At $t\delta = 0$, the chosen initial state is the superposition of two quantum register states. Here $n = 16$, $J/\delta = 0.4$ ($J/\delta > J_c/\delta = 0.22$), and one random realization is chosen.

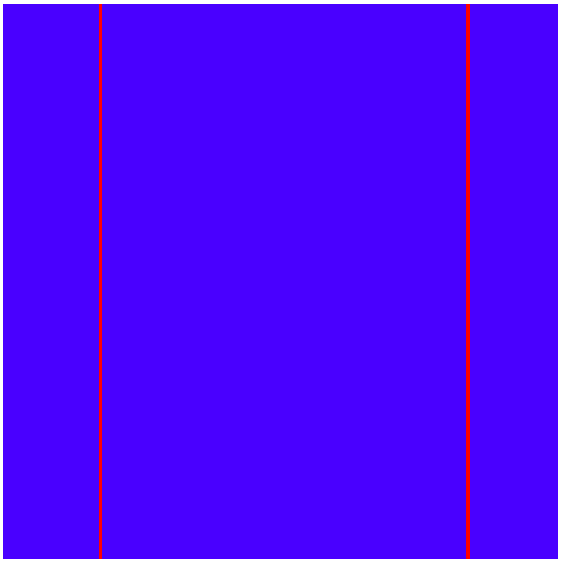

FIG. 18. Same as Fig.17 below the quantum chaos border, $J/\delta = 0.001$ ($J/\delta \ll J_{cs}/\delta = 0.026$).

The obtained data clearly show that exponentially many quantum register states become mixed after the finite chaotic time scale $\tau_\chi \approx 1/\Gamma$.

V. CONCLUSIONS

The results presented in this paper show that residual inter-qubit coupling can lead to quantum chaos and ergodic very complicated eigenstates of the quantum computer. We have shown that in this regime the quantum register states disintegrate quickly in time over an exponentially large number of states and the computer operability is destroyed. We determined the dependence of the chaotic time scale τ_χ of this process on coupling strength J, detuning fluctuations δ of one-qubit energy spacing, and number of qubits n. After this time τ_χ the quantum computer hardware is melt. To prevent this melting one needs to introduce an efficient error-correcting code which operates on a time scale much shorter than τ_χ and suppresses the development of quantum chaos. To avoid the quantum chaos regime dangerous for quantum computing, one should engineer the quantum computer in the integrable regime below the quantum chaos border $J_c \approx 3\delta/n$. It is important to note that this border decreases with the detuning δ, showing that imperfections do not all conspire against the operability of the computer. We stress again that the transition to quantum chaos is an internal process which happens in a perfectly isolated system with no coupling to external world. Nevertheless, since a decoherence can be viewed as a result of internal interactions in a larger system, the results presented here may also apply to this problem.

Our main conclusion is that although in the quantum chaos regime a quantum computer cannot operate for long, fortunately the border for this process happens to be exponentially larger than the spacing between adjacent computer eigenstates, and therefore a broad parameter region remains available for realization of a quantum computer. Another possibility is to operate the quantum computer in the regime of quantum chaos. However, here one should keep in mind that after the chaotic time scale τ_χ the computer hardware will melt due to inter-qubit coupling and quantum chaos. Therefor, the computer operability in this regime is possible only if many gate operations can be realized during the finite time τ_χ (in a sense it becomes similar to the decoherence time). It is clear that the most preferable regime corresponds to quantum computer operation below the quantum chaos border.

We thank O.P. Sushkov for stimulating discussions, and the IDRIS in Orsay and the CICT in Toulouse for access to their supercomputers. One of us (DLS) thanks the Gordon Godfrey foundation at the University of New South Wales at Sydney for the hospitality at the final stage of this work. This research is partially done in the frame of EC program RTN1-1999-00400.

---

* http://w3-phystheo.ups-tlse.fr/∼dima

[1] R. P. Feynman, Found. Phys. **16**, 507 (1986).
[2] D. P. Di Vincenzo, Science **270**, 255 (1995).
[3] A. Ekert and R. Josza, Rev. of Mod. Phys. **68**, 733 (1996).
[4] A. Steane, Rep. Progr. Phys. **61**, 117 (1998).
[5] D. Deutsch, Proc. R. Soc. London Ser. A **425**, 73 (1989).
[6] D. P. Di Vincenzo, Phys. Rev. A **51**, 1015 (1995).
[7] P. W. Shor, in Proc. 35th Annu. Symp. Foundations of Computer Science (ed. Goldwasser, S.), 124 (IEEE Computer Society, Los Alamitos, CA, 1994).
[8] L. K. Grover, Phys. Rev. Lett. **79**, 325 (1997).
[9] A. R. Calderbank and P. W. Shor, Phys. Rev. A **54**, 1098 (1996).
[10] A. Steane, Proc. Roy. Soc. Lond. A **452**, 2551 (1996).
[11] J. I. Cirac and P. Zoller, Phys. Rev. Lett. **74**, 4091 (1995).
[12] N. A. Gershenfeld and I. L. Chuang, Science **275**, 350 (1997); D. G. Cory, A. F. Fahmy and T. F. Havel, In Proc. of the 4th Workshop on Physics and Computation (Complex Systems Institute, Boston, MA, 1996).
[13] V. Privman, I. D. Vagner and G. Kventsel, Phys. Lett. A **239**, 141 (1998).
[14] B. E. Kane, Nature **393**, 133 (1998).
[15] C. D. Bowden and S. D. Pethel, Int. J. of Laser Phys., to appear (2000), (quant-ph/9912003).
[16] D. Loss and D. P. Di Vincenzo, Phys. Rev. A **57**, 120 (1998).
[17] Y. Nakamura, Yu. A. Pashkin, and J. S. Tsai, Nature **398**, 786 (1999).
[18] G. K. Brennen, C. M. Caves, P. S. Jessen and I. H. Deutsch Phys. Rev. Lett. **82**, 1060 (1999); D. Jaksch, H. J. Briegel, J. I. Cirac, C. W. Gardiner and P. Zoller, Phys. Rev. Lett. **82**, 1975 (1999).
[19] P. M. Platzman and M. I. Dykman, Science **284**, 1967 (1999).
[20] C. Monroe, D. M. Meekhof, B. E. King, W. M. Itano and D. J. Wineland, Phys. Rev. Lett. **75**, 4714 (1995).
[21] L. M. K. Vandersypen, M. Steffen, M. H. Sherwood, C. S. Yannoni, G. Breyta and I. L. Chuang, quant-ph 9910075.
[22] S. Haroche and J. M. Raimond, Phys. Today. 51 (august 1996).
[23] D. Mozyrsky, V. Privman and I. D. Vagner, cond-mat/0002350.
[24] C. Miquel, J. P. Paz and R. Perazzo, Phys. Rev. A **54**, 2605 (1996).
[25] C. Miquel, J. P. Paz and W. H. Zurek, Phys. Rev. Lett. **78**, 3971 (1997).
[26] J. B. French and S. S. M. Wong, Phys. Lett. B **33**, 449 (1970); O. Bohigas and J. Flores, *ibid* **34**, 261 (1971).
[27] S. Åberg, Phys. Rev. Lett. **64**, 3119 (1990).
[28] V. Zelevinsky, B. A. Brown, N. Frazier and M. Horoi, Phys. Rep. **276**, 85 (1996); V. V. Flambaum, F. M. Izrailev, and G. Casati, Phys. Rev. E **54**, 2136 (1996); V. V. Flambaum and F. M. Izrailev, Phys. Rev. E **56**, 5144 (1997).
[29] U. Sivan, F. P. Milliken, K. Milkove, S. Rishton, Y. Lee, J. M. Hong, V. Boegli, D. Kern, and M. de Franza, Europhys. Lett. **25**, 605 (1994).
[30] D. L. Shepelyansky and O. P. Sushkov, Europhys. Lett. **37**, 121 (1997).
[31] P. Jacquod and D. L. Shepelyansky, Phys. Rev. Lett. **79**, 1837 (1997).
[32] A. D. Mirlin and Y. V. Fyodorov, Phys. Rev. B **56**, 13393 (1997).
[33] B. Georgeot and D. L. Shepelyansky, Phys. Rev. Lett. **79**, 4365 (1997).
[34] D. Weinmann, J.-L. Pichard and Y. Imry, J. Phys. I France **7**, 1559 (1997).
[35] B. Georgeot and D. L. Shepelyansky, Phys. Rev. Lett. **81**, 5129 (1998).
[36] *Les Houches Lecture Series* **52**, Eds. M.-J. Giannoni, A. Voros and J. Zinn-Justin (North-Holland, Amsterdam, 1991).
[37] T. Guhr, A. Müller-Groeling and H. A. Weidenmüller, Phys. Rep. **299**, 189 (1999).
[38] B. Georgeot and D. L. Shepelyansky, quant-ph/9909074.
[39] A. Sørensen and K. Mølmer, Phys. Rev. Lett. **83**, 2274 (1999).
[40] This result is valid for short-range couplings. In the case of long-range couplings where all qubits are coupled, the system is similar to the one studied in [35], $\Delta_c \sim \delta/n^2$ and we will have $J_c \approx C'\delta/n^2$, where C' is a numerical constant.
[41] For even n and $\delta = 0$ the system has an additional symmetry corresponding to the inversion of all $\sigma_\mathbf{i} \to -\sigma_\mathbf{i}$ (spin inversion). However, inside one symmetry class the spacing statistics is still close to $P_W(s)$ according to our numerical data (not shown).
[42] E. P. Wigner, Ann. Math. **62**, 548 (1955); **65**, 203 (1957).
[43] V. V. Flambaum, quant-ph/9911061.